Multimed Tools Appl
DOI 10.1007/s11042-016-3302-9

An iterative closest point approach for the registration of volumetric human retina image data obtained by optical coherence tomography

Xin Wang[1,2] **· Zhen-Long Zhao**[1] **· Arlie G. Capps**[3] **· Bernd Hamann**[3]

Received: 7 May 2015 / Revised: 10 December 2015 / Accepted: 26 January 2016

Abstract This paper introduces an improved approach for the volume data registration of human retina. Volume data registration refers to calculating out a near-optimal transformation between two volumes with overlapping region and stitching them together. Iterative closest point (ICP) algorithm is a registration method that deals with registration between points. Classical ICP is time consuming and often traps in local minimum when the overlapping region is not big enough. Optical Coherence Tomography (OCT) volume data are several separate, partially overlapping tiles. To stitch them together is a technology in computer aided diagnosis. In this paper, a new 3D registration algorithm based on improved ICP is presented. First, the Canny edge detector is applied to generate the point cloud set of OCT images. After the detection step, an initial registration method based on the feature points of the point cloud is proposed to determine an initial transformation matrix by using singular value decomposition (SVD) method. Then, an improved ICP method is presented to accomplish fine registration. Corresponding point in the point cloud is weighted to reduce the iteration times of ICP algorithm. Finally, M-estimation is used as the objective function to decrease the impact of outliers. This registration algorithm is used to process human retinal OCT volume pairs that contain an overlapping region of $75 \times 500 \times 375$ voxels approximately. Then a comparative experiment is conducted on some public-available datasets. The experimental results show that the proposed method outperforms the classical method.

✉ Xin Wang
w_x@jlu.edu.cn

1 College of Computer Science and Technology, Jilin University, 130012 Changchun, China

2 Key Laboratory of Symbolic Computation and Knowledge Engineer of Ministry of Education, Jilin University, 130012 Changchun, China

3 Institute for Data Analysis and Visualization (IDAV), Department of Computer Science, University of California, Davis, Davis, CA 95616-8562, USA

Published online: 22 February 2016

Keywords Volume data registration · Optical coherence tomography · Retinal image · Iterative closest point · Point cloud

1 Introduction

Optical coherence tomography fundus images, which can provide high-resolution cross-sectional information of the human retina, are indispensable for clinical diagnosis, treatment and surgical evaluation of diseases such as macular degeneration and glaucoma. OCT processes high resolution in vivo volumetric imaging while the acquisition time is relatively short for avoiding motion artifacts caused by involuntary eye movement. Hence, the scan range of OCT is limited and only small volumetric data is acquired during one scan [23]. Therefore, it would be reasonable to focus on creating an OCT volume data covering a large field of view (FOV) [1].

Literatures on two-dimensional medical image registration are extensive [2, 16, 20]. Kratika Sharma and Ajay Goyal [21] made a survey of image registration techniques and provided overall source of recent as well as classic research. They divided image registration steps into four categories as spatial relations method, relaxation methods, pyramids and wavelets as well as methods using invariant descriptors. Mei-sen Pan et al. [18] proposed an image registration method based on edges that detected by the B-spline gradient operator. This method has a fairly simple implementation and it can be adapted to both mono-modality and multi-modality image registrations. Moreover, invariant descriptors can also serve in two-dimensional registration. Lucian Ciobanu and Luís Côrte-Real [7] provided a solution to register two complete-overlapped views problem based on iterative filtering of SIFT-generated key point matches, using the Hough transform and blocking matching. An iteration based approach was used to eliminate the most probable outlier and rebuilding the relations. It makes an overall significant reduction of the outliers while maintaining a high rate of correct matches. To achieve accurate and robust registration, another novel idea is modeling the entire image distribution. Shihui Ying et al. [24] first introduced this concept. Thus the procedure of groupwise registration is formulated as the dynamic shrinkage of graph on the manifold which brings the advantage of preserving the topology of the image distribution during the groupwise registration. Besides, some other feature based registration approaches can obtain satisfactory results [4, 15].

However, OCT volume data are composed of two dimensional B-scan images. Above registration methods may encounter difficulties in calculating memory and time limitation during process these volume. To register 3D OCT volume data, a novel idea to obtain a large FOV of OCT images is to create a montage [14]. In this method, blood vessel ridges are used as the feature of interest and a procedure based on resampling, interpolation, and cross-correlation is proposed to piece together the full OCT data. The montage method can integrate the dispersed, partially overlapping OCT images into a large 3D OCT image. However, this method would fail to register when blood vessel ridges are fuzzy. Other strategies generate a wide-field volume by using existing tools and platforms. Meng Lu [17] proposed an acceleration method based on Compute Unified Device Architecture (CUDA) which created by NVIDIA. This algorithm can improve the performance of 3D medical image registration and accelerate the calculation speed as well, which is suitable for large-scale data processing. Stephan Preibisch et al. [19] implement a stitching plugin in ImageJ that reconstructs several types of tiled microscopy acquisitions ranging from mosaics of histological 2D images to sets of gray-scale and RGB 3D confocal stacks. No prior knowledge is required and brightness differences between tiles are compensated by a smooth intensity transition. In addition to above these, some studies focus on stitching software and related stitching tools are developed successively [5, 10, 25]. However, some subtle non-rigid transformation appears during scan procedure due to the instability of ophthalmic instruments and involuntary eye movement. In hence these methods, which mainly deal with rigid transformation, have limitations in processing clinical ophthalmology OCT images.

In this paper, we focus on proposing a registration platform that can process non-rigid transformation and generate a large FOV of OCT volumetric data quickly and accurately. We use a coarse-to-fine strategy to calculate the transformation matrix which could integrate volumetric data together. First, edge points of each retinal image are selected by Canny edge detector and these edge points are collected together as point cloud. The purpose of Canny edge detector is to reduce the amount of points in point cloud and exclude the impact of noise. Then a method based on the feature points of point cloud is proposed to calculate the initial rough rigid registration matrix. Finally, the fine registration matrix is calculated by an improved ICP method. This method for global optimization could handle non-rigid transformation in its iterating step. Weighting method is taken into account when calculating the distance of each corresponding points. M-estimation object function is introduced to eliminate the abnormal points.

Our improved method accomplished 3D retinal OCT volume data registration and successfully broke through the efficiency bottleneck of volume registration. By comparison, time consumption and registration accuracy of our method are satisfactory.

The remainder of this paper is structured as follows. In the section 2, we give a details description of the proposed registration approach with the sub-sections 2.1, 2.2 and 2.3. The section 3 highlights the experiment implementation details and presents the results of the proposed approach on retinal OCT sub-volumes and some public-available datasets. Comparison with other registration method is made in the section 4 on a wide range of OCT datasets. Finally, a review of this paper and future work are presented in the section 5.

2 Materials and method

For the purpose of this paper, we use two 3D image sets as Reference Set and Target Set. Figure 1 shows these two sets. They are adjacent sub-volumes of human retina acquired by OCT instrument. We use a fundus image to show the actual position of the two sub-volumes.

The aim is to find out proper transformation matrixes to integrate all these sets into a full OCT volume data covering a large FOV. To begin with, the schematic of our algorithm is summarized as Fig. 2.

Canny method in first phase solved the problem of the large amount of data. In the initial registration phase, SVD method is used to decompose the feature points and eliminate the translation and rotation misalignment. Two constraints are added to improve the time consumption and registration accuracy of classical ICP method in Fine registration phase.

2.1 Generate point clouds of volumetric images

3D point clouds refer to a set of spatial data points and usually are used to represent the external surface of an object. Current commercial OCT instrument can obtain tiny volumetric

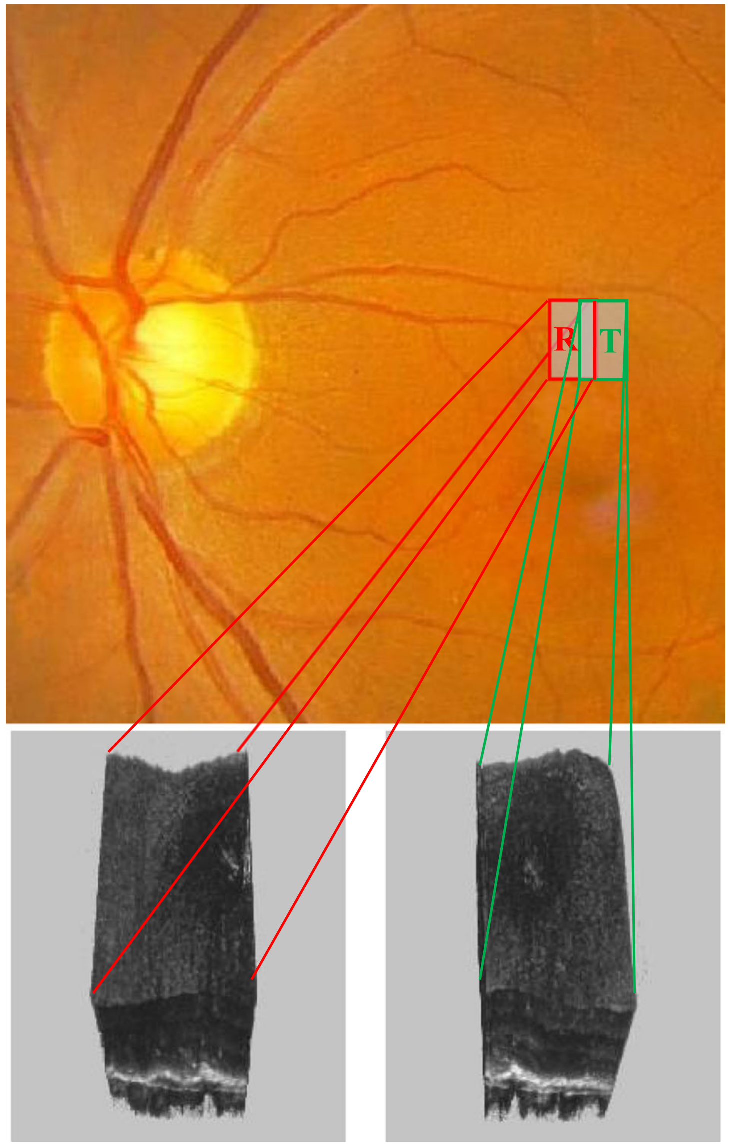

Fig. 1 The actual position of Reference Set (*left*) and Target Set (*right*). Fundus image is used for reference. Note that the two sets are adjacent human retina and composed by the superposition of single B-scan obtained by OCT instrument

images with high resolution. Generating point clouds by original OCT images will produce a huge amount of point clouds, which beyond the processing ability of current hardware and algorithms. Besides, during data acquisition procedure, there will generate approximately 0.1 %~5 % noise points. These noise points will affect registration process and result in accuracy decline. Thus, Canny method is used to detect the edge of retinal images, which helps to accelerate registration speed and reduce calculation amount. Canny method uses dual threshold to gather new edges in an 8-adjacement area, by which single noise point will not be treated as a part of edge. Besides, the edge detected by Canny method is the feature extraction of B-scans, which does not actually change the position information of the overlapping region of OCT volume, so using Canny method will lead to a good registration compared to original datasets. Figure 3 shows the result of a B-scan retinal image processed by Canny method.

Each pixel of the edge is regarded as a spatial point and all the edges of Reference Set and Target Set are adopted as the reference point cloud S_R and target point cloud S_T, respectively.

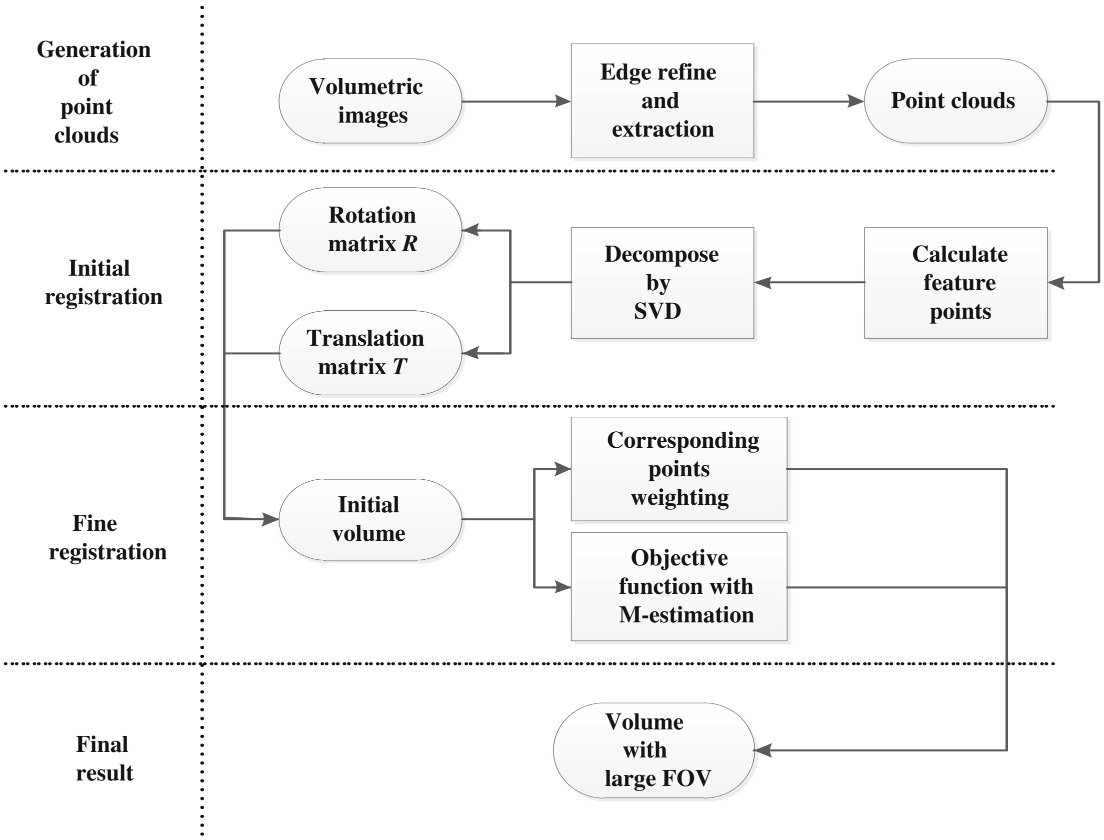

Fig. 2 Schematic diagram of the proposed algorithm. A coarse-to-fine transformation strategy is utilized to obtain OCT volume with large FOV

Canny edge detection eliminates the impact of noise and decreases the size of point cloud, thereby reducing the calculation burden of the numerous OCT fundus images.

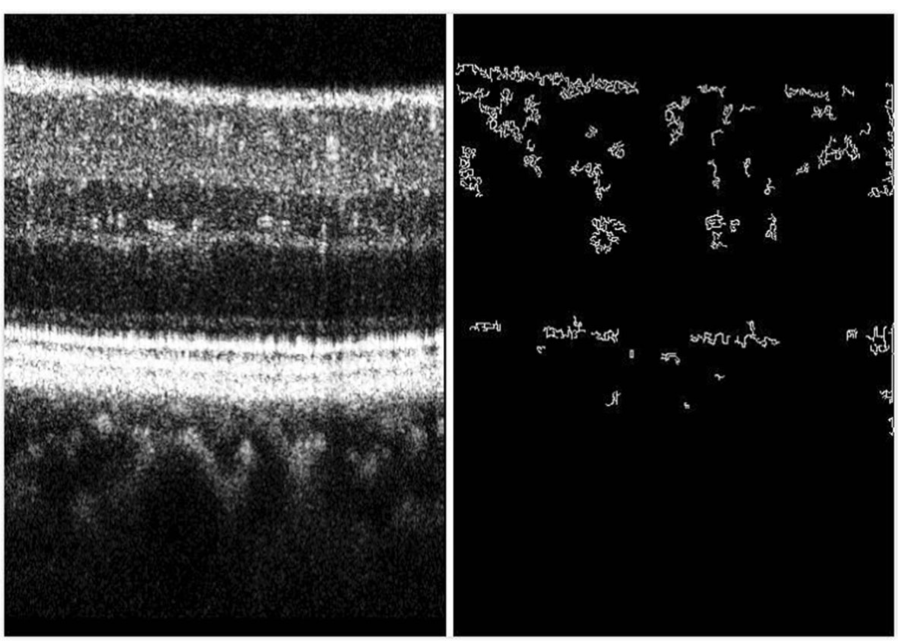

Fig. 3 Edge refine and extraction by Canny method (threshold $\lambda_1 = 300$, $\lambda_2 = 900$). The left image is a single B-scan retinal image acquired by OCT instrument, while the right shows the Canny edge of retinal image

2.2 Initial registration

We use a coarse-to-fine strategy to work out the transformation matrix, considering both registration results and efficiency. The purpose of initial registration is to eliminate the translation and rotation misalignment and provide a favorable initial state for fine registration. To this end, feature points are extracted from the two point cloud datasets and SVD method is utilized to work out the rotation matrix $\boldsymbol{R}$ and translation vector $\boldsymbol{T}$.

2.2.1 Extraction of feature points

To extract feature points, we first divide the point cloud sets into several spatial grids. Then we delineate all the boundary grids based on a novel selection algorithm. Finally, we split the boundary grids of point cloud and extract the feature points from these grids.

Oriented boundary box is used to find the minimum bounding box of point cloud datasets. Oriented boundary box is an oriented algorithm that makes the bounding box smallest. Different from axis-aligned bounding boxes, oriented boundary box is defined as a cuboid whose direction is arbitrary. After calculating the minimum bounding boxes of the two point cloud sets S_R and S_T, scaling transformation is used to ensure the two minimum bounding boxes a roughly equal size. Then, the size of spatial grids can be obtained from the minimum bounding box, which is defined as:

$$S_{grid} = K \bullet \frac{V}{Q} \tag{1}$$

where Q indicates the quantity of point cloud, V represents the volume of minimum bounding box. K is a variable parameter. For dense point cloud, experiments show that when K is assigned to be $8 \sim 24$, the size of spatial grid contains adequate points while will not be too large to affect registration accuracy. Let the size of spatial grid S_{grid} be K times of the reciprocal of the point cloud density and then divide the minimum bounding box equally spaced along the three axes according to this size. So far, all points in point cloud belong to certain grids according to their space coordinate. We define these spatial grids as occupied grid and empty grid according to whether contains points. Next, we extract the boundary grids using the following equation:

$$\begin{aligned} U(x,y,z) = f(x{-}1,y,z) \bullet f(x+1,y,z) + \\ f(x,y{-}1,z) \bullet f(x,y+1,z) + \\ f(x,y,z{-}1) \bullet f(x,y,z+1) \end{aligned} \tag{2}$$

where (x,y,z) is the spatial coordinate of a grid and $f(x,y,z)$ represents the type of a grid. If a grid is a occupied grid, $f(x,y,z) = 1$, otherwise $f(x,y,z) = 0$. A spatial grid (x,y,z) is classified as boundary grid or not by calculating its six adjacent neighbors. $U(x,y,z)$ is the sum of three products and each product value is 0 or 1. For example, if $f(x+1,y,z) \cdot f(x\text{-}1,y,z) = 1$, means that the left gird $(x+1,y,z)$ and the right grid $(x\text{-}1,y,z)$ of the current grid are both occupied grids. From the following figure (Fig. 4), we can conclude that a spatial grid (x,y,z) is a boundary grid when $U(x,y,z) \leq 1$,which represents there are no more than four adjacent neighbor grids are occupied grids. All boundary grids are selected by this method and each point in these grids is extracted as feature points.

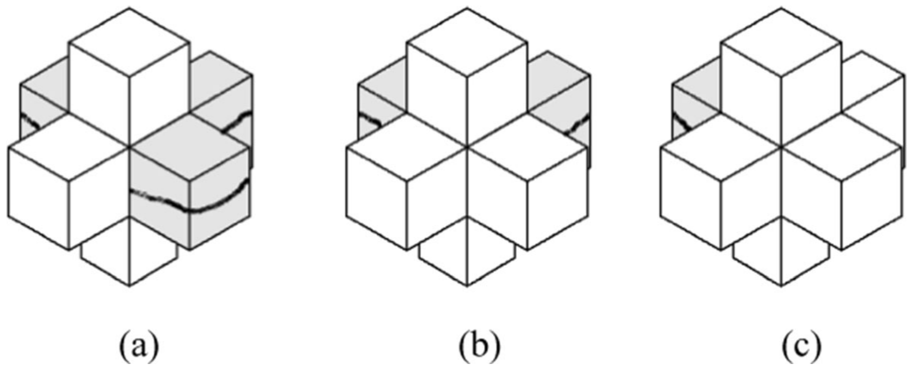

Fig. 4 Three cases of a boundary grid: **a** Boundary grid in a plane. **b** Boundary grid at the edge. **c** Boundary grid of vertex

2.2.2 Registration based on feature points

Once we have obtained the feature points, we gather them to participate in the initial registration. In our method, singular value decomposition is used to work out the rotation matrix $\boldsymbol{R}$ and translation vector $\boldsymbol{T}$ between corresponding pairs. A target matrix is defined by

$$E = \frac{1}{M}\sum_{i=1}^{M}(R_i - C_R) \times (T_i - C_T)^T \tag{3}$$

where C_R and C_T is the centroid of S_R and S_T respectively, M refers to the minimum number of points between S_R and S_T while R_i and T_i represents ith point in S_R and S_T. Decompose E by SVD, Eq. (3) reduces to $\boldsymbol{E} = \boldsymbol{UDV}^T$, the columns of $\boldsymbol{U}$ are the eigenvectors of the $\boldsymbol{EE}^T$ matrix and the columns of $\boldsymbol{V}$ are the eigenvectors of the $\boldsymbol{E}^T\boldsymbol{E}$ matrix. $\boldsymbol{V}^T$ is the transpose of $\boldsymbol{V}$ while $\boldsymbol{D}$ represents a diagonal matrix, by definition the non-diagonal elements are zero. $\boldsymbol{D} = diag(d_i)$ with $d_i \geq d_{i+1}$. Let

$$P = \begin{cases} I_3 & \det(U)\det(V) \geq 0 \\ diag(1, 1, -1) & \det(U)\det(V) < 0 \end{cases} \tag{4}$$

If $rank(\boldsymbol{P}) \geq 2$, then rotation matrix $\boldsymbol{R}$ can be calculated as $\boldsymbol{R} = \boldsymbol{UPV}^T$ and translation vector $\boldsymbol{T}$ can be calculated as $\boldsymbol{T} = C_T\text{-}\boldsymbol{R}C_R$. Apply $\boldsymbol{R}$ and $\boldsymbol{T}$ to S_R, we have finished the initial registration step.

2.3 Fine registration

Assume S_R and S_T contains N_R and N_T points respectively. Time complexity of classical ICP algorithm is $O(N_R \cdot N_T)$ ($O(N_R \cdot \log N_T)$ at best). When processing large volume data, massive time is spent on calculating the Euclidean distance between corresponding pairs. Another reason that makes classical ICP method unsuitable for our experiment is that it assumes the nearest point as corresponding point, which may trap the algorithm in local minimum. In this paper, an improved ICP method is proposed. First, all the corresponding points are weighted and those whose weight is smaller than a given threshold are eliminated. Second, M-estimation is introduced into the objective function to decrease the impact of abnormal points. In classical ICP algorithm, all the points are given an equal weight. In hence, each point in the point cloud will participate in the calculation of distance, which is the bottleneck of efficiency. In our method, a linked list is maintained which stores the effective points in distance calculation. Points are classified as effective points when their weight is larger than the threshold. We assume P_T is one point in S_T, the weight of P_T has the form:

$$weight = \frac{Dis_{MAX}}{Dis(P_R, P_T)} - 1 \tag{5}$$

where P_R is the current calculating point in S_R, $Dis(P_R,P_T)$ represents the Euclidean distance between P_R and P_T after initial registration step while Dis_{MAX} refers to the maximum distance between corresponding pairs. Effective points are stored in a linked list which will update after iterating a point. Points are excluded if their weights are smaller than a fixed threshold ε which is a variable argument that trades off time consumption and registration accuracy. If the threshold ε is decreased, the registration procedure would be more accurate but time consuming, which means there are more points should be processed as effective ones. And only effective points which are treated as corresponding points would participate in the calculation of Euclidean distance.

After excluding the points that have little effect on distance calculating, we introduce M-estimation to improve the objective function. M-estimation was proposed by Huber [12], which mainly deals with abnormal points. This method has overcome the shortcomings of traditional methods that may have no solution. M-estimation is the process of finding an estimate value X which makes the residual error smallest. Experiments show that it is likely to make registration trap into local minima when the number of abnormal points increases. In order to improve the robustness of registration algorithm, in this paper, a selecting weight iteration method proposed by Huber is used to reduce the sensitivity of the abnormal points. Huber defined the weighting factor of a point as:

$$\omega_\upsilon = \begin{cases} 1 & |\upsilon| \leq c \\ \dfrac{c}{\upsilon} & |\upsilon| > c \end{cases} \tag{6}$$

where ν means the residue of a point, c is a constant. In general, $c = 2\sigma$(σ is the standard deviation of a point in our algorithm). Huber M-estimation is a classical least squares estimation when ν range from $-c$ to c. Nevertheless, if residue ν is greater than c, the weighting factor decreases while residue increasing. Equation (7) shows the equation to calculate the Euclidean square distance of a corresponding pair A and B.

$$D_{AB} = \sqrt{\omega_X \bullet (X_A - X_B)^2 + \omega_Y \bullet (Y_A - Y_B)^2 + \omega_Z \bullet (Z_A - Z_B)^2} \tag{7}$$

We assume A, B are a corresponding pair of point cloud sets. ω_x, ω_y, ω_z represents the weighting factor of Huber M-estimation respectively while X_A, Y_A, Z_A, X_B, Y_B, Z_B refers to the spatial coordinates of A and B, respectively.

The process of our improved ICP algorithm is summarized as follow:

Given two point cloud sets S_R and S_T, an accuracy threshold τ, iterating the following steps:

- Exclude the points that have low weight according to a linked list (Initialized as empty).
- Calculate all Euclidean distance between the two sets from Eq. (7).
- For each point in S_R, find the nearest point in S_T as corresponding pairs and group them together as the nearest point set S_T^1.

– Calculate the translation vector $\boldsymbol{T}$ and rotation matrix $\boldsymbol{R}$ between S_R and S_T^1 using least mean square algorithm.
– Apply registration matrix $\boldsymbol{R}$ and $\boldsymbol{T}$ to S_R and get a new point cloud set S_R^1. Update the linked list and the root-mean-square error according to the new sets S_R^1 and S_T^1.

Until the root-mean-square error converges to the given threshold τ.

3 Experiments and results

In order to evaluate the registration performance of our proposed method, we conduct several experiments on both clinical datasets of human retinal OCT sub-volumes and public-available datasets. For the sake of comparison, we test our algorithm on different size of point cloud and discuss the experimental results.

Our proposed algorithm has been applied to process two retinal OCT sub-volumes, which are adjacent parts of the human retina structure. There are approximately 75 × 500 × 375 pixels overlapping region between the two sets. Figure 5 shows the iterating process from four different angles, the left visible area shows the initial position of the two point cloud (red points represent reference point cloud S_R and green points represent target point cloud S_T) while the right area indicates the real-time registration results of certain iteration step.

In our experiment, only the overlapping region of Reference Set and Target Set was selected to participate in the generation of point cloud considering the calculation time (177,489 cloud points after Canny method). The experimental result demonstrates a relatively accurate registration of OCT fundus volume data. Figure 6 shows the result of our method about the point cloud sets in detail, the left image demonstrates the relative position of the two OCT image sets. An obvious misalignment and some subtle deformation can be observed at zoom-in part. The proposed improved ICP method successfully registers the improper spatial cloud points which are illustrated by the right image in Fig. 6.

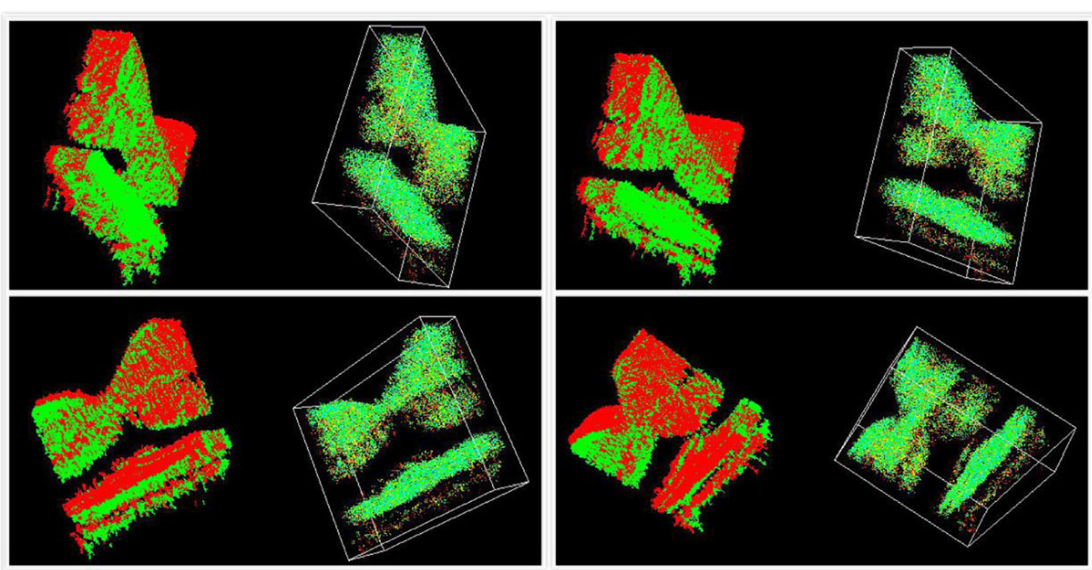

Fig. 5 Iterating process from different angles. The two point cloud sets are sampled as the left and the rights are real-time registration results. The cube profile on the right is the oriented boundary box of point cloud

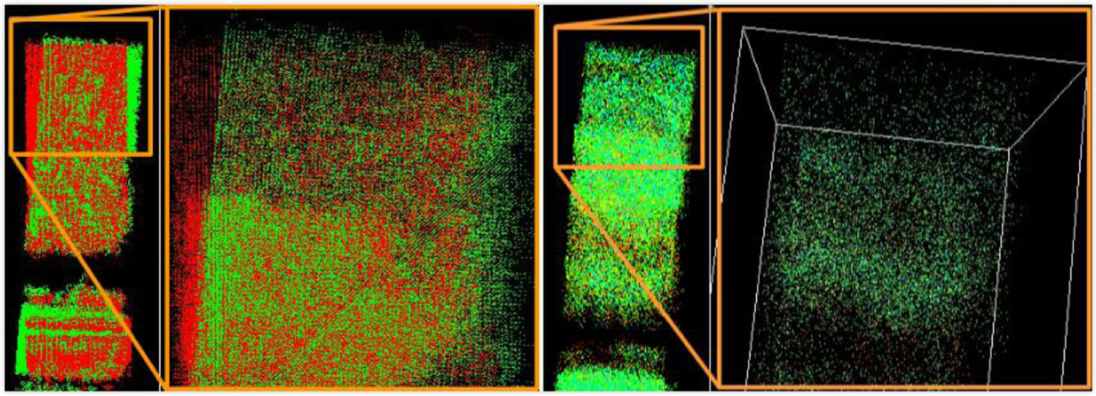

Fig. 6 Partially results of overlapping point cloud. The first image shows a zoom part of the overlapping region before registration, while the second shows the result of this part after using our method

The visualized experimental results are finally rendered by ImageJ. Figure 7 visualizes the initial experimental data sets as well as the experimental result. There are four rendered OCT volumes, the first two are experimental data that represent the Reference Set and Target Set mentioned above while the last two volumes on behalf of experimental result. Traditional registration of OCT volumes like that used in this paper may cause layer abruption especially in inner nuclear layer, photoreceptor cell layer and retinal pigment epithelium. However, the result images in Fig. 7 demonstrate a relative satisfactory retinal OCT volume. No obvious mosaic trace is found in our experimental result even at the overlapping region, thus the obtained volume with large FOV may better help clinicians in the prevention and diagnosis of ophthalmology disease.

As for the performance of registration method, there are no quantified standard with absolute certainty yet [8]. Researchers have proposed identification approaches from old and classical [11] to novel [9, 22]. In this paper, we utilize registration error to evaluate the performance, which is defined as:

$$\xi = 1 - \frac{\sum_{i=1}^{N} Success(P_R, P_T)}{N} \bullet 100\% \tag{8}$$

$Success(P_R,P_T)$ has the form:

$$Success(P_R, P_T) = \begin{cases} 1 & Dis(P_R, P_T) \leq \delta \\ 0 & Dis(P_R, P_T) > \delta \end{cases} \tag{9}$$

where N indicates the total number of corresponding pairs, (P_R,P_T) is a corresponding pair. $Success(P_R,P_T)$ indicates the registration result of corresponding pair (P_R,P_T). $Success(P_R,P_T) = 1$ when the Euclidean distance of the corresponding pair is smaller than the threshold δ. In the proposed performance evaluation formula (8), assuming that δ is 0.15 times of the original Euclidean distance of (P_R,P_T) before registration, which means all corresponding pairs whose Euclidean distance is less than 15 % of the original distance are successfully registered. Table 1 shows the time consumption and registration error of our algorithm and classical ICP algorithm proposed by Besl [3].

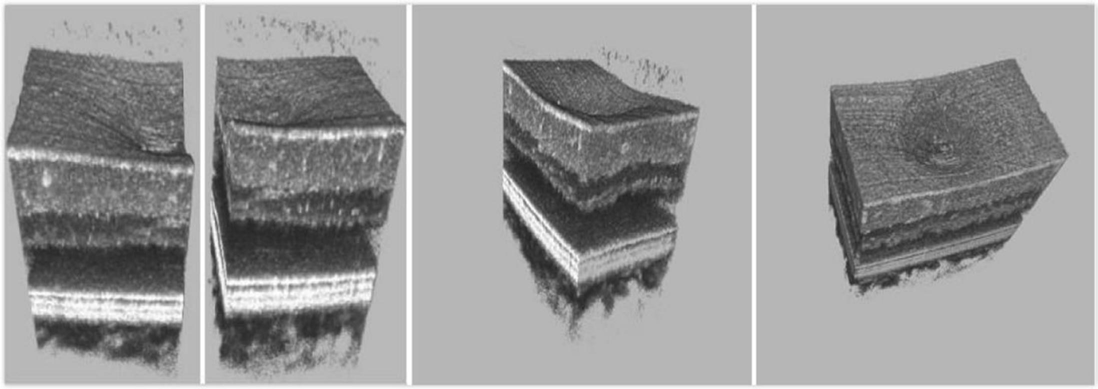

(a) (b) (c) (d)

Fig. 7 Experimental data and results rendered in ImageJ. After iterating the points of overlapping region, we got the transformation matrixes and applied them to Reference Set and Target Set. **a** The Reference Set of experimental data. **b** The Target Set of experimental data. **c** The side view of the result. This image shows the retinal layers situation after registration. **d** The top view of the result. This image shows the situation of fovea central is after registration

4 Discussion

With the development of OCT technique, 3D OCT volume data occupies an important place in computer-aided diagnose. Therefore, a satisfactory high-resolution OCT volume data with large FOV would be clinical desired. In this area, our team reached some results. Dae Yu Kim et al. [13] reported high-speed acquisition at 125 kHz A-scans with phase-variance OCT that could reduce motion artifacts and increase the scanning area. Arlie G. Capps et al. [6] described a method for combining and visualizing a set of overlapping volume images with high resolution but limited spatial extent. Robert J. Zawadzki et al. [26] presented a short review of adaptive optics OCT instruments and proposed a method for correcting motion artifacts in adaptive optics OCT volume data.

In this paper, we propose an algorithm to integrate 3D OCT datasets. There are some new features in our algorithm. Canny edge detector is applied to each OCT fundus image, which can remove the noise impact and reduce the calculation burden effectively (14,062,500 points of original overlapping region, 75 images, 375 × 500 pixels. 177,489 points after Canny edge detection method). In the initial registration step, spatial grid partition and singular value decomposition method is used to find out the matrix of rigid transformation which may cause by involuntary eye movement during data acquisition. The core of our method is the improved ICP algorithm. Points are weighted by their distance to the current corresponding point. Thus, the points that have low weight will not participate in the iteration step. Besides, M-estimation

Table 1 Comparison of experimental result

Registration method	Time consumption/s	Registration error
Classical ICP	308.881	0.00096834
Initial registration	8.623	–
Improved ICP	82.517	0.00020539

Illustration of stitching performance on tiled volumetric images computed on a Windows machine with Intel® 2-Core CPU (2.93 GHz). Single tile dimension is 75 × 500 × 375

Table 2 Different size of point cloud registration

Point cloud size	Time consumption Classical ICP /s	Time consumption Improved ICP /s
9731	11.023	3.994
28107	42.928	19.562
69670	150.447	41.090
177489	308.881	82.517
385316	512.848	123.962

is added to the equation that calculates the Euclidean square distance of corresponding pairs. There are three control parameters on x-axis, y-axis and z-axis respectively, which eliminate the impact of outliers and make the algorithm robust. Comparing with classical ICP algorithm, these new constraints made our method a less time consumption and better accuracy (Table 1). Our approach consumed 91.140 s totally in the experiment, which shortened a lot than classical ICP; the registration accuracy has considerable improvement as well. In the initial registration step, we eliminate the translation and rotation misalignment, which resulted in a larger overlapping region and fewer registration mistakes of corresponding points in the iterative process of ICP. Besides, the use of M-estimation also makes our approach more accurate. Weighting method is the core that makes our approach less time-consuming, which reduces the amount of points in the calculation of distance.

We also test our algorithm on different sets of point cloud including some public-available datasets. For example, the first point cloud in Table 2 is the "Stanford Bunny" after being processed by our method while the second one is the "Dragon" from The Stanford 3D Scanning Repository (http://graphics.stanford.edu/data/3Dscanrep/). Table 2 and Fig. 8 shows the performance of our improved ICP algorithm and classical ICP algorithm.

As is shown in Table 2 and Fig. 8, our method has obvious advantages when dealing with large volume data. In most cases, our algorithm increases the efficiency of classical

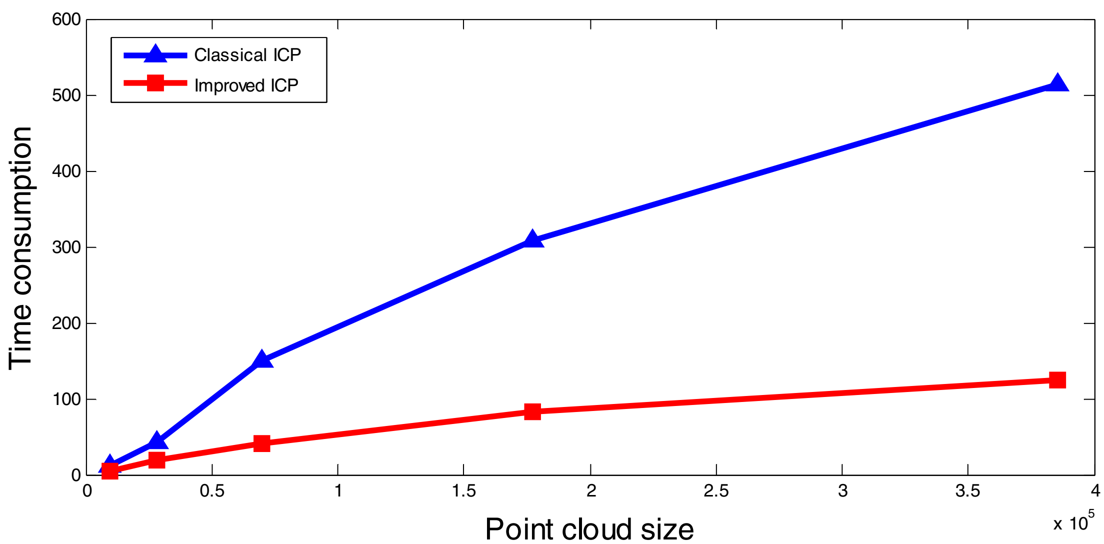

Fig. 8 Comparison of improved ICP with Besl's method in time consumption with different point cloud size. With data size growing, our improved method stands out

ICP algorithm by 70 %. Above analysis demonstrates the effectiveness of our method and the possibility to apply it to process other OCT datasets that can be transformed into point clouds.

5 Conclusion

We present a non-rigid registration method of OCT retinal images, which can generate a 3D ocular fundus volume covering a large FOV. Canny edge detection method has been applied in the first stage of the proposed method to generate the point cloud. Oriented boundary box is used to process the point cloud set and obtain the feature points. The initial registration matrix is calculated based on these feature points and SVD method. At last, an improved ICP algorithm is proposed to work out the fine registration matrix between the point cloud sets. Several human retinal OCT image sets and some public-available datasets are used to test the performance of the proposed method. The experimental results show the performance of our algorithm has an obvious improvement compared with classical ICP algorithm in terms of time consumption and registration accuracy. In clinical practice, there are several partially overlapping OCT volumes of human retina. Under the same coordinate system, each volume has a fixed coordinate. So after registering of two volumes, we regard them as a new volume and integrate it with other volumes. The proposed method could provide strong support for clinical treatment and diagnosis. Our future work will focus on a self-adapted strategy to register OCT sub-volumes automatically.

Acknowledgments This work was supported by the National Natural Science Foundation of China (No. 60905022) and the Jilin Provincial Research Foundation for Basic Research, China (No. 201105016). We thank the members of the Institute for Data Analysis and Visualization (IDAV) at the University of California, Davis. We also thank Jack Werner and Robert Zawadzki of the Vision Science and Advanced Retinal Imaging Laboratory at the University of California, Davis.

References

1. Assayag O, Antoine M, Sigal-Zafrani B et al (2014) Large field, high resolution full field optical coherence tomography: a pre-clinical study of human breast tissue and cancer assessment. Technol Cancer Res Treat 13:455–468
2. Ayyachamy S, Manivannan VS (2013) Medical image registration based retrieval using distance metrics. Int J Imaging Syst Technol 23:360–371
3. Besl PJ, McKay ND (1992) Method for registration of 3-D shapes. Robotics-DL tentative. Int Soc Opt Photon 586–606
4. Biswas B, Dey K N, Chakrabarti A (2015) Medical image registration based on grid matching using Hausdorff Distance and Near set. 2015 I.E. Eighth International Conference on Advances in Pattern Recognition (ICAPR)1–5
5. Bria A, Silvestri L, Sacconi L et al (2012) Stitching terabyte-sized 3D images acquired in Confocal Ultramicroscopy. 2012 9th IEEE International Symposium on Biomedical Imaging (ISBI): 1659–1662. doi:10.1109/ISBI.2012.6235896
6. Capps AG, Zawadzki RJ, Werner JS et al (2013) Combined volume registration and visualization. Vis Med Life Sci, Proc 7–11. doi: 10.2312/PE.VMLS.VMLS2013.007-011
7. Ciobanu L, Côrte-Real L (2011) Iterative filtering of SIFT keypoint matches for multi-view registration in Distributed Video Coding. Multimed Tools Appl 55:557–578
8. Cohen EAK, Ober RJ (2013) Analysis of point based image registration errors with applications in single molecule microscopy. IEEE Trans Signal Process 6291–6306

9. Datteri RD, Liu Y, D'Haese P et al (2014) Validation of a non-rigid registration error detection algorithm using clinical MRI brain data. IEEE Trans Med Imaging 34:86–96
10. Emmenlauer M, Ronneberger O, Ponti A et al (2009) XuvTools: free, fast and reliable stitching of large 3D datasets. J Microsc 233:42–60
11. Hemler PF, Napel S, Sumanaweera TS et al (1995) Registration error quantification of a surface-based multimodality image fusion system. Med Phys 22:1049–1056
12. Huber PJ (2009) Robust statistics, 2nd edn. Wiley, Hoboken
13. Kim DY (2011) In vivo volumetric imaging of human retinal circulation with phase-variance optical coherence tomography. Biomed Opt Express 2:1504–C1513
14. Li Y, Gregori G, Lam BL et al (2011) Automatic montage of SD-OCT data sets. Opt Express 19:26239–26248
15. Li Y, Stevenson R (2014) Incorporating global information in feature-based multimodal image registration. J Electron Imaging 23(2):76–85. doi:10.1117/1.JEI.23.2.023013
16. Liu B, Zhang B, Wan C et al (2014) A non-rigid registration method for cerebral DSA images based on forward and inverse stretching–avoiding bilinear interpolation. Bio-Med Mater Eng 24:1149–1155
17. Meng L (2014) Acceleration method of 3D medical images registration based on compute unified device architecture. Bio-Med Mater Eng 24:1109–1116
18. Pan M, Jiang J, Rong Q et al (2014) A modified medical image registration. Multimed Tools Appl 70:1585–1615
19. Preibisch S, Saalfeld S, Tomancak P (2009) Globally optimal stitching of tiled 3D microscopic image acquisitions. Bioinformatics 25:1463–1465
20. Riffi J, Mahraz AM, Tairi H (2013) Medical image registration based on fast and adaptive bidimensional empirical mode decomposition. IET Image Process 7:567–574
21. Sharma K, Goyal A (2013) Classification based survey of image registration methods. Int Conf Comput Commun Netw Technol 1–7
22. Surucu M, Roeske J (2013) A novel metric to evaluate dose deformation error for deformable image registration algorithms. Med Phys. doi:10.1118/1.4814322
23. Vignali L, Solinas E, Emanuele E (2014) Research and clinical applications of optical coherence tomography in invasive cardiology: a review. Curr Cardiol Rev 10:369–376
24. Ying S, Wu G, Wang Q, et al (2013) Groupwise registration via graph shrinkage on the image manifold. IEEE Conf Comput Vis Pattern Recogn 2323–2330
25. Yu Y, Peng H (2011) Automated high speed stitching of large 3D microscopic images. Biomedical Imaging: From Nano to Macro. 2011 I.E. International Symposium on IEEE:238–241
26. Zawadzki RJ, Capps AG, Kim DY et al (2014) Progress on developing adaptive optics–optical coherence tomography for in vivo retinal imaging: monitoring and correction of eye motion artifacts. IEEE J Sel Top Quantum Electron 20:7100912

Xin Wang master's supervisor, Female, born in 1975, received the PhD degree in computer science and technology from Jilin University in 2006. She worked in Jilin University from 1999. She also worked in University of California, Davis from 2011 to 2012 as a visiting scholar. Her research interests include image processing, computer graphics, bioinformatics and computational biology.

Zhen-Long Zhao Male, born in 1990, received the B.S. degree in software college from Jilin University, Changchun, China, in 2013. He is currently pursuing the master degree in computer science and technology at Jilin University. His research interests include image processing, computer graphics and bioinformatics.

Arlie G. Capps Male, received the B.S. degree in computer science from Brigham Young University, Provo, UT, USA, in 2004. He is currently pursuing the Ph.D. degree in computer science at the University of California, Davis, CA, USA. He is a Livermore Graduate Scholar at Lawrence Livermore National Laboratory. His research interests include scientific and medical volume visualization, multimodal data fusion, and error quantification and correction.

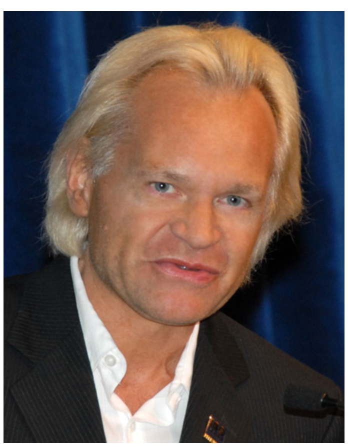

Bernd Hamann Male, teaches computer science at the University of California, Davis. His main areas of interest are data visualization, geometric design and computing, and computer graphics. He studied mathematics and computer science at the Technical University of Braunschweig, Germany, and at Arizona State University, Tempe, U.S.A.